Few-cycle vector solitons of light

A. V. Kim and S. A. Skobelev
Institute of Applied Physics, Russian Academy of Sciences, 603950 Nizhny Novgorod, Russian Federation
(Received 26 July 2010; revised manuscript received 16 May 2011; published 23 June 2011)

We present a class of few-cycle elliptically polarized solitary waves in an isotropic Kerr medium. It is proved numerically that they are stable and can be easily excited during pulse propagation. We also propose a method of producing multisolitons with different polarization states and study their binary collisions. It is shown that collisional properties strongly depend on their relative polarization rotation.

DOI: 10.1103/PhysRevA.83.063832 PACS number(s): 42.65.Tg

I. INTRODUCTION

The recent progress in laser science has established a new field of "extreme light" where very short laser pulses comprising only a few optical cycles interact with matter (see, e.g., [1,2]). It is expected that such few-cycle laser pulses could shed new light on nonlinear physics, ranging from ultrabroadband nonlinear optics [3] through attosecond science [4] and from relativistic nonlinear optics to nonlinear quantum electrodynamics [5]. Another important area where few-cycle pulses occur is terahertz radiation [6].

One of the most striking effects in nonlinear physics is the existence of solitary waves; in particular, in the extreme nonlinear optics these are few-cycle solitons, which result from the interplay between dispersion and nonlinearity. Such localized waves, known as optical solitons in conventional nonlinear optics [7], play an exceptionally important role in various areas of physics [8]. In particular, vector or elliptically polarized solitons represent a very important class of localized solutions as the nonlinear birefringence induced by the optical Kerr effect becomes significant and polarization evolution is altered drastically [9]. This is also highly important, because elliptically polarized pulses can provide a new dimension of laser parameters that allows quantum control in molecules and nanostructures [10,11]. However, in the few-cycle regime exact soliton solutions were found only recently for linear [12] and circular [13] polarization of light. Moreover, the basic wave equation for the linearly polarized field belongs to the class of completely integrable equations. It is important to notice that in the limiting case of shortest durations there is a qualitative difference in the condition of existence of these two types of solitons (see below) and therefore the existence of such few-cycle solitons with arbitrary polarizations states is not trivial.

In this paper we provide an important link between the linearly and circularly polarized solitons by finding the so-called few-cycle elliptically polarized solitary waves in an isotropic Kerr medium. These solitons are characterized by a fixed polarization ellipse that uniquely rotates at a constant rate over the propagation distance. Such a rotation is quite similar to the case of Schrödinger-like solitons in nonbirefringent media [14,15]. From our point of view this looks very surprising, since in the conventional nonlinear optics, where the slowly varying envelope approximation (SVEA) is used, there is no qualitative difference between linearly and circularly polarized solitons. It is worth noting that an elliptically polarized vector soliton (Schrödinger-like) in an isotropic Kerr medium was recently observed experimentally [15]. We also reveal novel physics of nontrivial interaction between these solitons and show that their interaction crucially depends on relative polarization rotations.

II. BASIC WAVE EQUATION

In general, the vector wave equation for isotropic media with Kerr nonlinearity can be written in the following form (see, e.g., [16]):

$$\partial_z^2 \mathbf{E} - \frac{1}{c^2}\partial_t^2 \int_{-\infty}^{t} \varepsilon(t-t')\mathbf{E}(t')dt' = \frac{4\pi}{c^2}\partial_t^2 \mathbf{P}_{nl}, \qquad (1)$$

$$\partial_t \mathbf{P}_{nl} = g(\mathbf{E}^2\partial_t \mathbf{E}) + h[\mathbf{E},[\mathbf{E},\partial_t \mathbf{E}]] = 0, \qquad (2)$$

where $\partial_{i=z,t}$ stands for the respective derivatives, ε is the isotropic linear permittivity, and g, h are the parameters of instantaneous Kerr nonlinearity. The response time of the nonlinearity is assumed to be instantaneous. In the optical region of transparency, the Fourier representation of the linear permittivity can be taken in the form $\varepsilon(\omega) = \varepsilon_o - a/\omega^2 + b\omega^2$, where the frequency-dependent terms are usually very small compared to the static dielectric permittivity of the medium ε_o, i.e., $a/\omega^2, b\omega^2 \ll \varepsilon_o$ [13,17]. In the particular case of electronic-type Kerr nonlinearity ($h = 2g/3$), by employing the slowly evolving wave approximation [16], which assumes the pulse profile only to be slowly varying on a distance comparable with its duration, we can arrive at a reduced wave equation for a real electric field with arbitrary light polarization (see, e.g., [13,18]), which we write in the following form

$$\partial_\tau\left[\partial_z U - \mu\partial_\tau^3 U + \partial_\tau(|U|^2 U)\right] + U = 0, \qquad (3)$$

where $U = (E_x + iE_y)(4\pi\chi^{(3)}/a)^{1/2}$ is a new complex variable and $\chi^{(3)} = 5g/3$ is the cubic nonlinear susceptibility (see, e.g., [16]); a new propagation coordinate $z \to za/(2c\varepsilon_o^{1/2})$, and retarded time $\tau = t - z\varepsilon_o^{1/2}/c$ are introduced, where c is the speed of light in vacuum; and the parameter $\mu = b/a$ accounts for the type of dispersion: if $\mu = 0$ ($b = 0$), anomalous dispersion takes place in the whole spectral interval.

III. FEW-OPTICAL-CYCLE SOLITONS

Paying particular attention to the case of anomalous dispersion ($\mu = 0$) where few-cycle solitons can exist and assuming solutions of Eq. (3) in the form

$$U(z,\tau) = A(z,\tau)e^{i\varphi(z,\tau)}, \qquad (4)$$

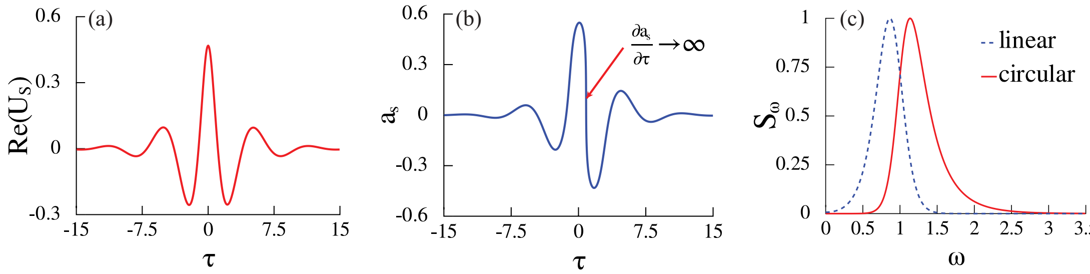

FIG. 1. (Color online) Temporal profile of few-cycle shortest-duration solitons for (a) circularly and (b) linearly polarized fields, and their spectra (c). All quantities normalized as in the text.

we obtain for real functions $A(z,\tau)$ and $\varphi(z,\tau)$ the following set of equations:

$$A_{z\tau} - A\varphi_z\varphi_\tau + A + (A^3)_{\tau\tau} - A^3\varphi_\tau^2 = 0, \tag{5}$$

$$A\varphi_{z\tau} + A_z\varphi_\tau + A_\tau\varphi_z + 2(A^3)_\tau\varphi_\tau + A^3\varphi_{\tau\tau} = 0. \tag{6}$$

The type of polarization is now defined by $\varphi(z,\tau)$. The two limiting cases of linear and circular polarization, where exact soliton solutions for few cycles are found, are now well developed. For the simplest case of circular polarization, the soliton solutions of Eqs. (5) and (6) can be represented as [13]

$$A(z,t) = \gamma^{1/2}A_S(\xi), \tag{7}$$

$$\varphi(z,\tau) = \omega(\tau + \gamma z) + \Phi_S(\xi), \tag{8}$$

$$\Phi_S(\xi) = \int_{-\infty}^{\xi} \frac{A_S^2(3 - 2A_S^2)}{2(1 - A_S^2)^2} d\xi', \tag{9}$$

where $\xi = \omega(\tau - \gamma z)$, ω is the soliton carrier frequency, and γ^{-1} is the soliton group velocity. The intensity profile $A_S(\xi)$ is a solitonlike solution of the second-order ordinary differential equation for the stationary envelope distribution taking place at $\delta^2 = 1/\gamma\omega^2 - 1 \leqslant \delta_c^2 = 1/8$. It should be noted that the existence of the limiting soliton with the shortest duration is defined by the constraint $\int_{-\infty}^{\infty} U d\tau = 0$, which is one of the integrals of Eq. (3): at $\delta = \delta_c$ the shortest duration is equal to $\tau_s^* = 2.31\omega^{-1}$.

The limiting circularly polarized soliton and its spectrum are depicted in Fig. 1(a). The case of linear polarization corresponds to $\varphi(z,\tau) = const = \varphi_o$, where the vector of electric field makes an angle φ_o with the x axis. In this case Eq. (3) without loss of generality can be reduced to one equation for $A(z,\tau)$ with $\varphi = 0$, which at $\mu = 0$, as was shown in Ref. [12], is an integrable equation that may be rewritten through a chain of transformations as a sine-Gordon equation. Thus starting from breather solutions of the sine-Gordon equation we can obtain an exact form of linearly polarized solitons. Note that there is a qualitative difference between linearly and circularly polarized solitons. It comes from the fact that for solitons with linear polarization in the limiting case of the shortest duration the first time derivative of the field $[a_s(z,\tau)]_\tau \to \infty$, i.e., shock-wave formation occurs in the field profile [see Fig. 1(b)]. We would like to emphasize this point, indicating that self-steepening of the real field profile is much more efficient for linearly polarized pulses, whereas for circularly polarized pulses it occurs over the intensity profile only. However, it is worth noting that the spectrum of the soliton with circular polarization is broader than with the linear one, as is clearly seen in Fig. 1(c). This occurs because of strong self-phase modulation over the intensity profile for the circularly polarized field, which is reflected in the solution of Eq. (9). This means that, in general, linearly polarized solitons cannot be represented as a pair of counter-rotating circularly polarized solitons, unlike the case of vector solitons described by two coupled nonlinear Schrödinger equations [14].

Let us now try to identify pulses with polarizations other than circular or linear ones that propagate as solitary waves. We have performed numerical studies in this intermediate regime to prove the existence of elliptically polarized solitary waves and their stability as well. To solve Eq. (3) we use the split-step Fourier method in which the spatial and temporal steps were chosen as $\Delta z = 0.02$ and $\Delta\tau = 0.115$ in order to provide conservation of the Hamiltonian of Eq. (3),

$$H = \int_{-\infty}^{+\infty} \left[\frac{|U|^4}{2} + \mu|\partial_\tau U|^2 - \left| \int_{-\infty}^{\tau} U d\tau \right|^2 \right], \tag{10}$$

with the accuracy of 10^{-5} (the number of points over time is 2^{14}).

Our starting point is the analytical solutions for solitons with circular polarization given by Eqs. (7) and (8) that are used as the initial condition. Indeed, if the input field distribution is represented in the form of Eqs. (7) and (8) but with different amplitudes of the (x,y)-field components, i.e.,

$$\mathrm{Re}(U) = \gamma^{1/2}A_S(\tau)\cos\varphi_s \tag{11}$$

$$\mathrm{Im}(U) = (1-\epsilon)\gamma^{1/2}A_S(\xi)\sin\varphi_s\ , \tag{12}$$

any elliptically polarized solitary wave can be easily excited during pulse propagation. In such an input pulse there are actually two governing parameters: soliton amplitude or δ and ϵ, allowing proper excitation of the elliptically polarized soliton with given ellipticity.

A typical example of a single elliptically polarized soliton excitation is shown in Fig. 2, where the input parameters are $\omega = 1$, $\delta = 0.32$, and $\epsilon = 0.95$. Linear dispersion length for these parameters is $L_d \simeq 15$. In this case, after a transient stage when part of pulse energy is emitted in the form of continuous waves, a solitary wave is formed with a duration of about 1.5 optical cycles and polarization ellipse with ellipticity of about 0.95 uniquely rotating along the propagation distance, for which a longitudinal period of ellipse rotation is about $L \simeq 1536$.

Another problem of fundamental as well as of practical interest is generation of predictable multisoliton pulses with

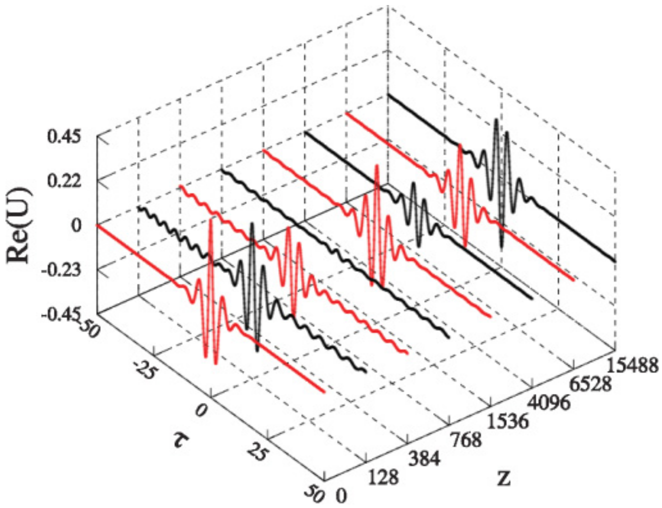

FIG. 2. (Color online) Single elliptically polarized soliton excitation with input pulse parameters $\omega = 1$, $\delta_{in} = 0.32$, and $\epsilon_{in} = 0.95$. After a transient stage a few-cycle soliton with ellipticity 0.95 is formed. Linear dispersion length for these parameters is $L_d \simeq 15$. All quantities normalized as in the text.

different polarization states. Since we now know how to generate a single elliptically polarized solitary wave, it is natural to use the concept of higher-order solitons, which plays an exceptionally important role in the theory of the nonlinear Schrödinger equation and has been used for optical pulse compression of circularly polarized pulses down to single-cycle duration [13]. Indeed, by introducing the higher-order soliton number N as a parameter and defining an initial field distribution in the form $U(z = 0, \tau) = NU_S$, where U_S is the solitonlike solution of Eq. (3) with a given polarization state (see above), it is really possible to produce $[N]$ soliton pulses $[[N]$ is the integer of $N]$. As an example, Fig. 3 shows the dynamic evolution of a solitonlike pulse with $N = 2$, $\delta = 0.1$, and $\epsilon = 0.9$. As is seen from this simulation, the first significant pulse compression occurs at $z \simeq 500$, which is similar to the Schrödinger scenario of higher-order soliton propagation, except for the fact that essential asymmetry appears in the field profile and this is due to the nonlinear group velocity effect. Further, the pulse decays and eventually two solitary waves are formed with different polarization states. The rate of ellipse rotation, as was to be expected, is higher for intense solitons and they rotate in one direction. Thus the concept of higher-order solitons gives a meaningful prediction of the number of generated solitons, but the drawback of this procedure is that there is no regular recipe of generating solitons with needed polarization ellipticity.

IV. THE ROLE OF HIGH-FREQUENCY DISPERSION ($\mu \neq 0$)

The next important issue in terms of feasibility of solitons with elliptic polarization is their dynamics, taking into consideration the high-frequency component of medium dispersion ($\mu \neq 0$) that we have neglected before. It is known that introduction of the fourth derivative into Eq. (3) may change the dispersive properties significantly, in particular, there may appear a point of zero group velocity dispersion $\omega_{cr} = (3\mu)^{-1/4}$.

With the high-frequency dispersion taken into account, all the mentioned properties of elliptically polarized solitons were retained when the wave pattern spectrum was in the region $\omega < \omega_{cr}$. The main question here is what happens if a substantial part of the pulse spectrum is in the region with normal group velocity dispersion. The evolution of the wave field specified at the input to the nonlinear medium as an elliptically polarized soliton shown in Fig. 2 for $\mu = 0.08$ is illustrated in Fig. 4. For the given parameters, ω_{cr} is 1.43, so that the point of zero group velocity dispersion is at the high-frequency end of the pulse spectrum [Fig. 4(b)]. Clearly, for the chosen parameters about 15% of the optical pulse energy is initially in the region with normal group velocity dispersion [see Fig. 4(b) for $z = 0$]. As was to be expected, this leads to division of the initial spectrum into two parts: the right-hand part of the spectrum

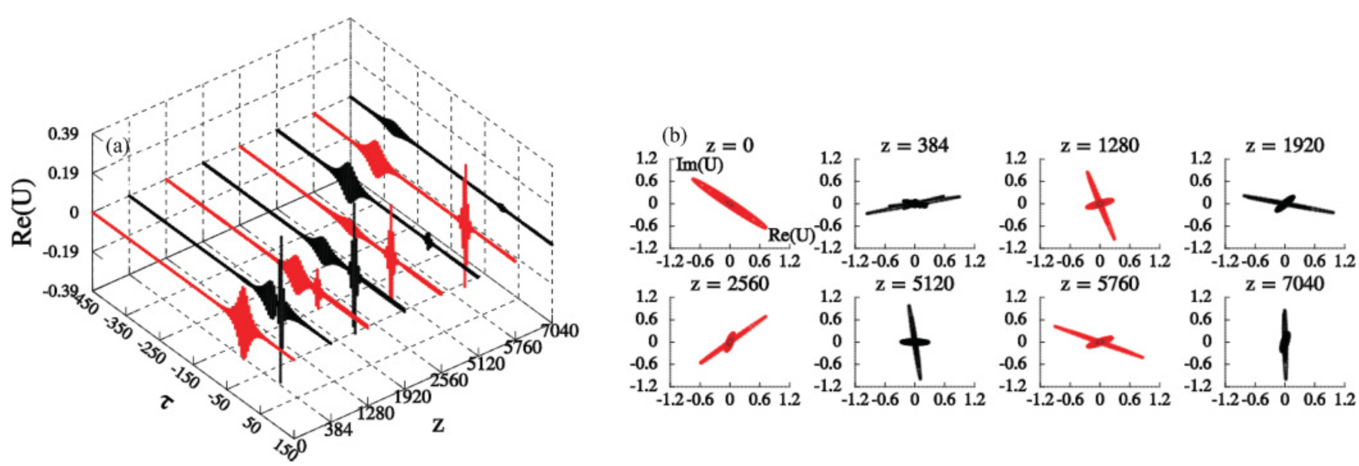

FIG. 3. (Color online) Evolution of elliptically polarized pulse during propagation for the case of an input pulse in the form of a higher-order soliton with $N = 2$, $\delta = 0.1$, $\epsilon = 0.9$, and $\omega = 1$: (a) temporal profiles of x-field component and (b) snapshots of polarization ellipse at different propagation distances. Two output solitons are generated with ellipticities of about $\epsilon_1 \simeq 0.96$ and $\epsilon_2 \simeq 0.8$. Their polarization ellipses rotate with the periodicity along the propagation direction equal to $L_1 \simeq 1984$ and $L_2 \simeq 4288$. All quantities normalized as in the text.

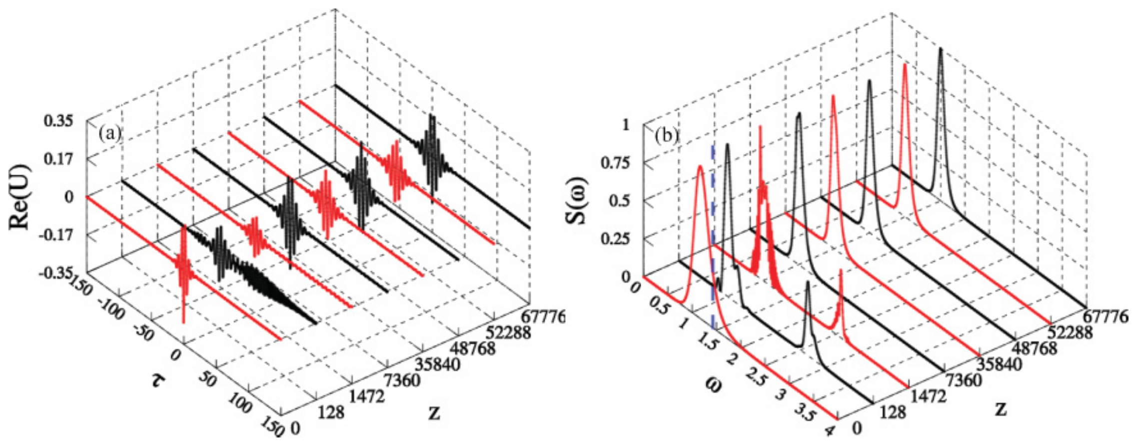

FIG. 4. (Color online) Snapshots of field distribution (a) and spectrum (b) along the propagation distance. Input pulse is a few-cycle soliton with $\omega_{in} = 1$ and $\delta_{in} = 0.32$; $\omega_{cr} = 1.43$, $\epsilon = 0.95$. Dispersion length for these parameters is $L_d \simeq 15$. The blue dashed line shows the position of the point of zero group velocity dispersion. All quantities normalized as in the text.

($\omega > \omega_{cr}$) is emitting into traveling quasiharmonic waves, and the left-hand side transforms into a new solitonlike structure with a small number of field oscillations, but shifted by the carrier frequency to the red (low-frequency) spectral region. Further, the newly formed soliton propagates without changes (Fig. 4). It is worth noting that the spectrum of the formed structure is fully localized in the region with anomalous group velocity dispersion [Fig. 4(b)]. Numerical simulation demonstrates formation of a soliton having ellipticity $\epsilon \simeq 0.95$ and period of rotation of the principal axis of polarization ellipse $L \simeq 4608$.

The emission of quasiharmonic waves having an isolated spectrum in the shorter wavelength region has been actively studied as a route to broadband blue-light generation in microstructured fibers and mostly attributed to the so-called fiber-optic Cherenkov radiation (see, e.g., [19] and references therein). However, it should be mentioned that when a soliton is formed nothing is emitted into the normal region of the spectrum. Only on the transient stage of pulse propagation is the presence of the parametric interaction between the soliton and continuous waves indicated by the appearance of an isolated peak [around 2.5 as in Fig. 4(b)], which then disappears as a result of group pulse spreading (in the numerical scheme the pulse goes beyond the time limits of the computations). The energy efficiency of parametric frequency conversion at $z = 128$ is about 26% [see Fig. 4(b)].

With a further shift of the central frequency of a few-cycle soliton to the point of zero dispersion, part of the soliton spectrum is in the region with the normal law of group velocity dispersion ($\omega > \omega_{cr}$), leading to stronger modification of the solitonlike pulse generated. Note that if the central frequency is in the region of normal dispersion and is close to the point of zero group velocity dispersion ω_{cr}, effective generation of the spectral continuum occurs that is accompanied by pulse spreading in the time domain. Nevertheless, a soliton of longer duration may be also formed in this case too, as soon as part of the initial pulse spectrum is localized below the critical frequency, in conformity with recent experiments [20]. Figure 5 demonstrates results of computer simulations, showing the dependence of the effective soliton generation on ω_{cr} [Fig. 5(b)]. The average duration $\langle\tau\rangle$ and average frequency $\langle\omega\rangle$ of the formed soliton are shown in Fig. 5(c) and 5(d), respectively. As the process of soliton formation is accompanied by emission of waves into a continuous spectrum, this leads to longer average soliton duration. As follows from Fig. 5(c), for the parameters corresponding to Fig. 4, the average pulse duration increased 2.1 times ($\langle\tau_{\text{out}}\rangle \simeq 2.1\langle\tau_{in}\rangle$) and the average soliton frequency decreased 1.22 times ($\langle\omega_{\text{out}} \simeq 1.22\langle\omega_{in}\rangle$). Note that Fig. 5 highlights two things: stable generation of solitons with a small number of field oscillations, and energy efficiency of this process. Thus solitons with a small number of field oscillations may be readily excited in a wide parameter region and, hence, may be regarded to be elementary structures that play a fundamental role in dynamics of short optical pulses.

V. BINARY-COLLISION DYNAMICS

It is well known that the result of binary soliton collisions (see, e.g., [8]) is a very important sign of the fundamental property of integrability of the basic equation. To shed light on the dynamics of the collisions we focused special attention on the circularly polarized solitons, particularly the ones rotating in opposite directions, and carried out simulations of Eq. (3), where we scanned input parameters of the soliton-soliton interactions with different amplitudes, carrier frequencies, and polarization states.

Since Eq. (3) describes unidirectional pulse propagation, for studying soliton collisions the soliton with lower group velocity was placed ahead of the other one. By summarizing results of the simulation, we can conclude that soliton-soliton collisions have several distinct features. First, the most prominent feature is that the interaction strongly depends on their relative rotation directions. As was shown in Ref. [21], if colliding solitons rotate in one direction, there are three different regimes of the interaction, depending on the absolute phase difference of the colliding pulses: (1) the solitons pass through each other, (2) they are reflected completely, and (3) the solitons exactly replicate each other during interaction.

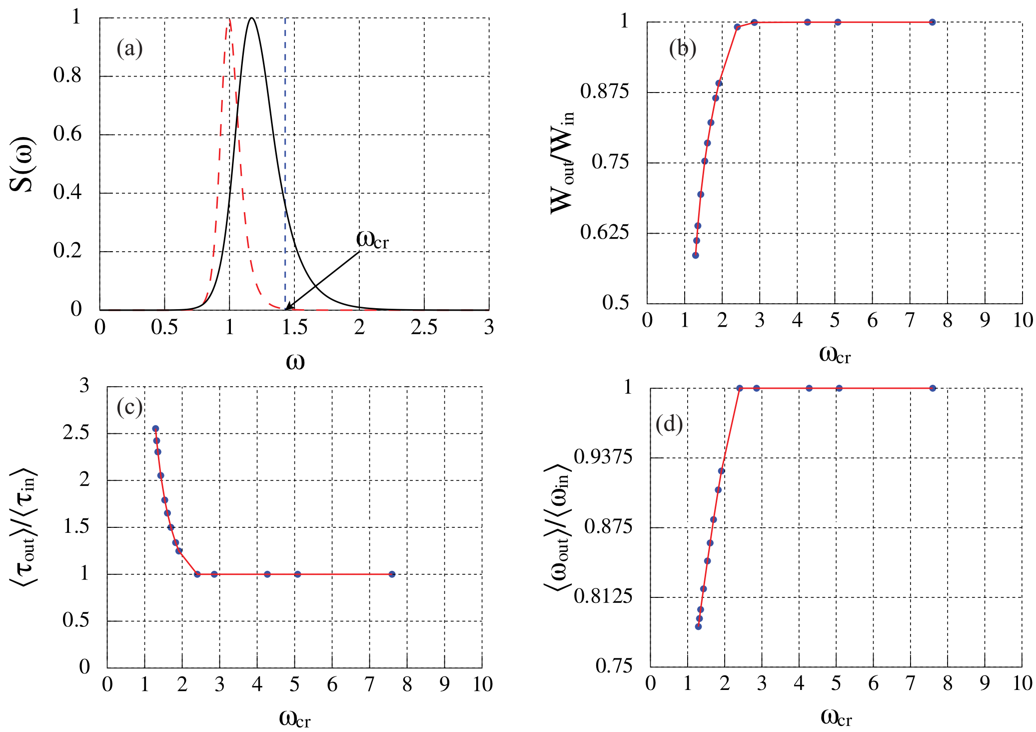

FIG. 5. (Color online) (a) Wave soliton spectral power $S(\omega)$ at the input $z =$ (solid black curve) and for $z = 67\,776$ (red dashed curve), corresponding to Fig. 4. The blue dashed curve denotes position of the point of zero group velocity dispersion. The spectra are normalized to unity. (b) The dependence of the ratio of generated pulse energy to input pulse energy as a function of ω_{cr}; (c) average soliton duration $W \cdot \langle\tau\rangle = \int \tau |U|^2 d\tau$ as a function of ω_{cr}, where W is pulse energy; (d) average carrier frequency $W \cdot \langle\omega\rangle = \int \omega \cdot S(\omega) d\omega$ of the formed soliton as a function of ω_{cr}. Soliton energy, average carrier frequency, and average soliton duration are normalized to the corresponding initial values. All quantities normalized as in the text.

However, if soliton carrier frequencies are different and/or incident amplitudes differ by more than 40%, only one regime is realized: the solitons pass through each other without any changes. It is worthy of notice that their interactions are quite close to the interactions of the Schrödinger solitons.

A qualitatively different situation occurs when colliding solitons rotate in opposite directions, i.e., assuming $\mathrm{Re}(U) = \gamma_1^{1/2} A_{S1} \cos\varphi_{s1} + \gamma_2^{1/2} A_{S2} \cos\varphi_{s2}$ and $\mathrm{Im}(U) = \gamma_1^{1/2} A_{S1} \sin\varphi_{s1} - \gamma_2^{1/2} A_{S2} \sin\varphi_{s2}$, where $\gamma_1, A_{S1}, \varphi_{s1}, \gamma_2, A_{S2}, \varphi_{s2}$ are parameters of two colliding solitons and their solutions of Eqs. (7) and (8). In this case, the result of the collision strongly depends on the difference between the carrier frequencies. If they are equal, as shown, for example, for the soliton parameters $\delta_1 = 0.05, \delta_2 = 0.1$, $\omega_1 = \omega_2 = 1$ in Fig. 6(a), solitons elastically (to an accuracy of simulation) reflect each other in the sense that no continuous waves are really emitted during the interaction. The important argument is that we can control modeling of Eq. (3) with high precision, since it has the Hamiltonian $H = \int_{-\infty}^{\infty} [|U|^4/2 + \mu |U_\tau|^2 - |\int_{-\infty}^{\tau} U d\tau|^2] d\tau$, which is very sensitive to an accuracy of simulation, and additional control is also made by using another constant of motion — the total energy $W = \int_{-\infty}^{\infty} |U|^2 d\tau$.

Thus this case of collision strongly differs from the colliding solitons rotating in one direction when they pass through each other without energy exchange. We assume that in this case, since permittivity is modulated with double carrier frequency (or spatially at half the incident wavelength), the effective Bragg reflection occurs, leading to complete reflection of the solitons by each other. However, if the incident wave frequencies are notably different, the colliding solitons pass through each other without energy losses [as is clearly seen in Fig. 6(c)]. In the intermediate case, when the soliton frequencies differ by no more than 5%, they interact inelastically, i.e., continuous waves are emitted during the interaction process and the solitons can lose a substantial part of their energies, as is shown in Fig. 6(b) for the incident soliton parameters $\delta_1 = 0.05, \delta_2 = 0.1$, $\omega_1 = 0.98$, and $\omega_2 = 1.02$, when about 10% of the incident soliton energies is emitted by linear waves.

VI. CONCLUSION

To conclude, we have found a novel family of solitary waves in an isotropic Kerr medium — few-cycle, elliptically polarized solitons which play a central role in the polarization dynamics of optical pulse propagation. We have proved that these solitons are stable and can be easily excited by a proper choice of input pulses. The scheme of multisoliton generation with different polarization states based on the extension of the higher-order Schrödinger solitons to the few-cycle regime with elliptically polarized pulses has been proposed. For clarification of the basic properties of vector few-cycle solitons, we have paid specific attention to their binary collisions and revealed that the collision properties

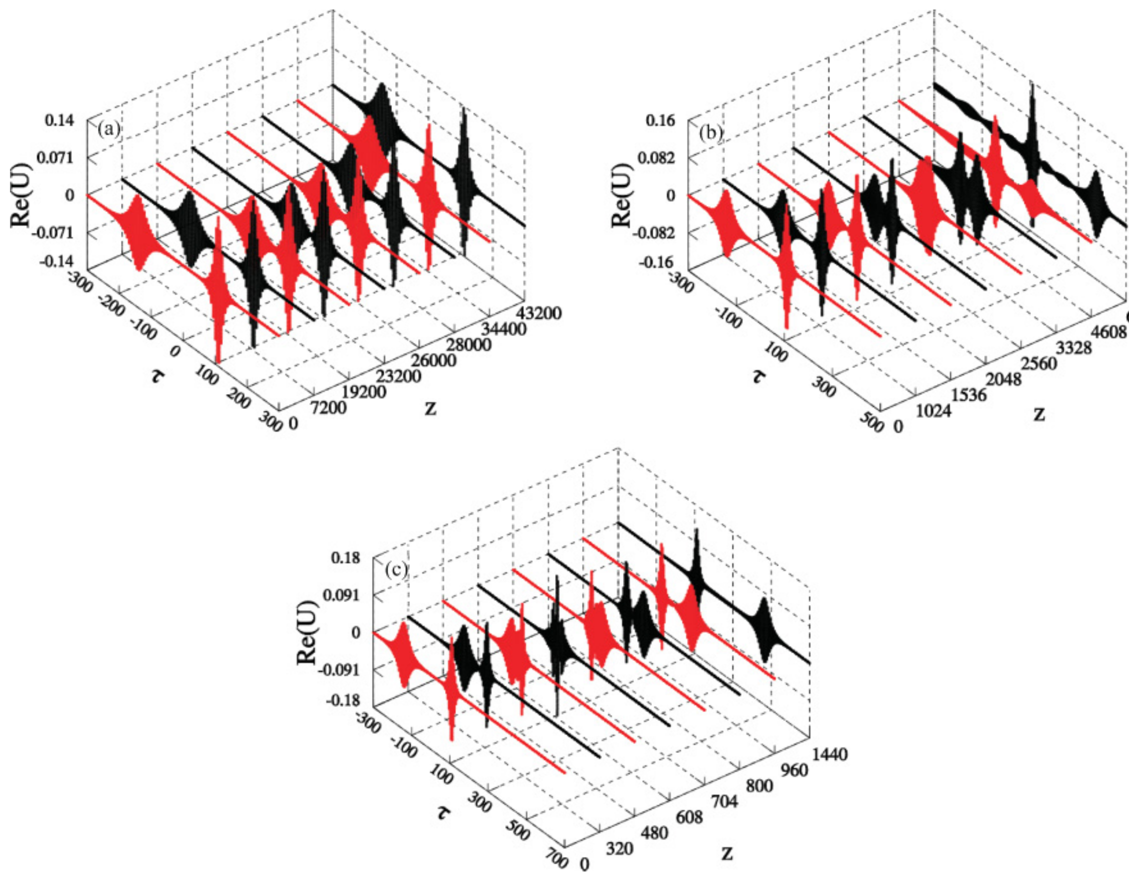

FIG. 6. (Color online) Snapshots of field distributions of colliding pulses with polarization ellipses rotating in opposite directions (a) when carrier frequencies are equal and the pulses elastically reflect each other; (b) when carrier frequencies are different with $\omega_1 = 0.98$, $\omega_2 = 1.02$, and the pulses interact inelastically, emitting about 10% of the incident soliton energies by linear waves; and (c) when carrier frequencies are different with $\omega_1 = 0.9$, $\omega_2 = 1.1$ and the pulses interact elastically. All quantities normalized as in the text.

strongly depend on their relative polarization rotation. If they rotate in one direction, the solitary waves interact with each other, persisting to be solitons in the sense of unit intensity envelope structure similar to the Schrödinger solitons, whereas with opposite ellipse rotation they always reflect each other or interact inelastically.

ACKNOWLEDGMENTS

This work was partially supported by the Russian Foundation for Basic Research through Grants No. 10-02-00596 and No. 10-02-01400. One of authors (S.A.S.) also acknowledges partial support from the RF President Grant No. MK-4902.2011.2 and "Dynasty" Foundation.

[1] M. Wegener, *Extreme Nonlinear Optics* (Springer-Verlag, Berlin, 2005).
[2] G. A. Mourou, T. Tajima, and S. V. Bulanov, Rev. Mod. Phys. **78**, 309 (2006).
[3] J. M. Dudley, G. Genty, and S. Coen, Rev. Mod. Phys. **78**, 1135 (2006).
[4] A. Baltuška *et al.*, Nature (London) **421**, 611 (2003).
[5] M. Marklund and P. K. Shukla, Rev. Mod. Phys. **78**, 591 (2006).
[6] J. Dai, X. Xie, and X.-C. Zhang, Phys. Rev. Lett. **97**, 103903 (2006).
[7] Yu. S. Kivshar and G. P. Agrawal, *Optical Solitons: From Fibers to Photonic Crystals* (Academic, New York, 2003).
[8] R. K. Dodd, J. C. Ellbeck, J. D. Gibbon, and H. C. Morris, *Solitons and Nonlinear Wave Equations* (Academic, London, 1982).
[9] H. G. Winful, Opt. Lett. **11**, 33 (1986).
[10] Y. Silberberg, Nature (London) **430**, 624 (2004).
[11] J. Itatani, D. Zeidler, J. Levesque, M. Spanner, D. M. Villeneuve, and P. B. Corkum, Phys. Rev. Lett. **94**, 123902 (2005).
[12] A. Sakovich and S. Sakovich, J. Phys. A **21**, L361 (2006).
[13] S. A. Skobelev, D. V. Kartashov, and A. V. Kim, Phys. Rev. Lett. **99**, 203902 (2007); A. V. Kim *et al.*, Phys. Rev. A **77**, 043823 (2008).
[14] M. Haelterman and A. P. Sheppard, Phys. Lett. A **194**, 191 (1994); Y. Silberberg and Y. Barad, Opt. Lett. **20**, 246 (1995).
[15] M. H. Delqué *et al.*, Opt. Lett. **30**, 3383 (2005); M. Delque, G. Fanjoux, and T. Sylvestre, Phys. Rev. E **75**, 016611 (2007).
[16] T. Brabec and F. Krausz, Rev. Mod. Phys. **72**, 545 (2000).
[17] L. D. Landau and E. M. Lifshitz, *Electrodynamics of Continuous Media* (Pergamon, New York, 1960).

[18] S. A. Kozlov and S. V. Sazontov, JETP **84**, 221 (1997); V. G. Bespalov, S. A. Kozlov, Y. A. Shpolyansky, and I. A. Walmsley, Phys. Rev. A **66**, 013811 (2002).

[19] G. Chang, L.-J. Chen, and F. X. Kärtner, Opt. Express **19**, 6635 (2011).

[20] E. E. Serebryannikov, A. M. Zheltikov, N. Ishii, C. Y. Teisset, S. Kohler, T. Fuji, T. Metzger, F. Krausz, and A. Baltuska, Phys. Rev. E **72**, 056603 (2005).

[21] S. A. Skobelev and A. V. Kim, JETP Lett. **80**, 623 (2004).